

Spectra and cycle structure of trophically coherent graphs

Samuel Johnson^{1,*} and Nick S. Jones²

¹*Warwick Mathematics Institute, and Centre for Complexity Science,
University of Warwick, Coventry CV4 7AL, United Kingdom.*

²*Department of Mathematics, Imperial College London, SW7 2AZ, United Kingdom.*

We analyse the spectral properties of generic directed graphs and find that a single parameter, τ – a function of ‘trophic coherence’ and the correlation between the in- and out-degrees of vertices – determines which of two regimes a given network falls into. In one there is a divergent number of cycles and leading eigenvalues are large. In the other, the probability of a randomly drawn graph being acyclic tends to unity, and leading eigenvalues have vanishing real parts. Thus, the value of τ will determine many kinds of behaviour in complex systems – such as spreading processes, dynamical stability and synchronization – which are related to graph spectra or feedback loops. Our theory is in good agreement with empirical data for several classes of network, and may explain certain non-trivial properties of biological systems, such as the prevalence of ‘qualitatively stable’ networks.

PACS numbers: 89.75.Fb, 89.75.Hc, 05.40.-a, 05.90.+m

Physicists have been interested in the eigenspectra of random matrices ever since Eugene Wigner first used them to model the energy levels of heavy atoms [1]. When the matrices in question are taken to represent graphs, or networks, their eigenvalues can be related to fundamental questions regarding both structure [2, 3] and dynamical processes – such as percolation [4], stability of dynamical elements [5], diffusion [6], or synchronization of coupled oscillators [7]. It has recently been shown that the particularly high linear stability of the interaction matrices related to food webs is determined mainly by a structural feature called ‘trophic coherence’, a measure of how neatly vertices fall into distinct levels [8]. However, the effects of trophic coherence on generic directed graphs have yet to be explored. To this purpose we define the ‘coherence ensemble’ and obtain expressions for the cycle structure and for spectral properties of the adjacency matrix in terms of trophic coherence. We find that the key ingredient is a parameter τ which determines which of two regimes a given network belongs to. In one, leading eigenvalues are large and the number of directed cycles of length ν grows exponentially with ν ; in the other, all eigenvalues have real parts close to zero, and graphs have few cycles. In fact, the probability of drawing a directed acyclic graph in this regime tends to one with decreasing τ . The expected value of the leading eigenvalue, in either regime, is simply $\overline{\lambda}_1 = e^\tau$.

Consider the directed, unweighted graph given by the $N \times N$ adjacency matrix $A = (a_{ij})$, which has $L = \sum_{ij} a_{ij}$ directed edges. The in- and out-degrees of vertex i are $k_i^{\text{in}} = \sum_j a_{ij}$ and $k_i^{\text{out}} = \sum_j a_{ji}$, respectively, and the mean degree is $\langle k \rangle = L/N$ (we shall use the notation $\langle \cdot \rangle$ to refer to averages over elements in a given graph, as opposed to ensemble averages). The eigenspectrum of A is $\{\lambda_i\}$. The distribution of eigenvalues, $p(\lambda)$, is related to powers of A via its moments: $\text{Tr}(A^\nu) = N\langle \lambda^\nu \rangle$. Since A is not, in general, symmetric, its eigenspectrum will be complex. The trace of A is real and invariant with

respect to a change of basis, so the eigenvalues of A will always be distributed symmetrically around the real axis. Of particular interest is the eigenvalue with largest real part, λ_1 – usually referred to as A ’s leading eigenvalue.

A ‘basal vertex’ is one with in-degree equal to zero. If a graph has at least one basal vertex, and every vertex belongs to at least one directed path which includes a basal vertex, we can define the trophic level of each vertex i as $s_i = 1 + \frac{1}{k_i^{\text{in}}} \sum a_{ij} s_j$. [8]. With no loss of generality for subsequent results, we define the trophic level of basal vertices as $s_i = 1$, as is the convention in ecology. The ‘trophic distance’ associated to each edge is $x_{ij} = s_i - s_j$ (note that this is not strictly a distance, since it can take negative values). The distribution of trophic distances $p(x)$ has mean $\langle x \rangle = 1$ by definition, and we can measure the graph’s ‘trophic coherence’ with the standard deviation $q = \sqrt{\langle x^2 \rangle - 1}$. A graph will be more trophically coherent the closer q is to zero.

The number of directed paths (henceforth ‘paths’) of length ν in A is $n_\nu = \sum_{ij} (A^\nu)_{ij}$. The number of directed cycles (henceforth ‘cycles’) of length ν is $m_\nu = \text{Tr}(A^\nu)$, which can be expressed as $m_\nu = N\langle \lambda^\nu \rangle$. (Note that we are not referring here to simple paths and simple cycles, in which no vertex can be repeated.) This definition of m_ν counts every unique cycle ν times, so the number of unique cycles will be $m_\nu^u = m_\nu/\nu$.

The directed configuration ensemble is the set of graphs with given sequences of in- and out-degrees [9]. Using this ensemble as a null-model, we can obtain the expected numbers of paths and cycles by inserting the expected value of the adjacency matrix for large graphs, $\tilde{a}_{ij} = k_i^{\text{out}} k_j^{\text{in}} / L$, in the above definitions (we shall use the notation \tilde{z} to refer to the expected value of a magnitude z in the directed configuration ensemble). Thus, the expected number of paths in this ensemble is $\tilde{n}_\nu = L\alpha^{\nu-1}$, while the expected number of those paths which are cycles is $\tilde{m}_\nu = \alpha^\nu$, where $\alpha \equiv \langle k^{\text{in}} k^{\text{out}} \rangle / \langle k \rangle$ captures the correlation between the in- and out-degrees of vertices.

We can also obtain a mean-field estimate for the trophic coherence of graphs in the directed configuration ensemble. If there are B basal vertices, the mean trophic level will be $\tilde{s} = B/N + \tilde{s}_{nb}(N - B)/N$, where \tilde{s}_{nb} is the expected level of a node given that it is not basal. From the definition of trophic levels, and assuming average levels for the neighbours of each non-basal node, we can write $\tilde{s}_{nb} = \tilde{s} + 1$. Combining these equations we have $\tilde{s} = N/B$ and $\tilde{s}_{nb} = 1 + N/B$.

The edges can be separated into two sets: those which emanate from basal vertices, and those which do not. The expected trophic distance will be $\tilde{x} = s_{nb} - 1$ for edges in the first set, and $\tilde{x} = 0$ for those in the second. The distribution of trophic distances is thus bimodal and, when the separation of the two modes is much larger than the spread about them, it can be approximated by $p(\tilde{x}) = BN^{-1}\delta(\tilde{x} - N/B) + (1 - B/N)\delta(\tilde{x})$. The trophic coherence associated with this distribution is $\tilde{q} = \sqrt{N/B - 1}$. In Supplemental Material (SM) we measure the trophic coherence of networks generated with the directed configuration model and power-law in- and out-degree distributions, and of directed versions of Erdős-Rényi random graphs. We give numerical evidence that \tilde{q} provides a good estimate in each case, irrespective of the heterogeneity of in- and out-degree distributions.

The coherence ensemble. Let us now consider the ensemble of graphs which not only have given in- and out-degree distributions (as in the directed configuration ensemble), but also given trophic coherence. We shall refer to this as the *coherence ensemble*, and use the notation $E(z) = \bar{z}$ for the expected values of magnitudes z in this ensemble. For networks in the coherence ensemble, the probability that a randomly chosen path of length ν be a cycle can be obtained by considering a random walk along the edges of the graph and computing the probability that it return to the initial vertex after ν hops. This constraint implies that the sum of the trophic distances x_k over the $k = 1, \dots, \nu$ edges involved, $S = \sum_k x_k$, be equal to zero. Let us approximate the distances x_k as independent random variables drawn from the distribution $p(x)$. According to the central limit theorem, the distribution $p(S)$ will tend, with increasing ν , to a Gaussian with mean $\nu\langle x \rangle = \nu$ and variance νq^2 . Since cycles are paths which satisfy $S = 0$, the expected proportion of paths of length ν that are cycles, \bar{c}_ν , will be proportional to $p(S = 0)$. That is, $\bar{c}_\nu = B_\nu \exp[-\nu/(2q^2)]/(\sqrt{\nu}q)$. Not all the paths satisfying $S = 0$ will return to the initial vertex, and this effect is accounted for by the factor B_ν . We can obtain B_ν by considering the configuration ensemble case, for which we know both c_ν and q , and where $\bar{c}_\nu = \bar{m}_\nu/\bar{n}_\nu = \alpha/L$. Equating this with the expression for \bar{c}_ν , we obtain $B_\nu = \alpha L^{-1} \sqrt{\nu} \tilde{q} \exp[\nu/(2\tilde{q}^2)]$. Therefore, the general expression for \bar{c}_ν is

$$\bar{c}_\nu = \frac{\alpha \tilde{q}}{L} \exp\left[\frac{\nu}{2} \left(\frac{1}{\tilde{q}^2} - \frac{1}{q^2}\right)\right]. \quad (1)$$

The expected proportion of paths of size ν which are cycles can thus either decrease or increase exponentially with ν , depending on whether a particular graph is more or less trophically coherent than the null expectation given its degree sequence. Eq. (1) was obtained using the central limit theorem, and so should only be valid for moderately large ν . However, if the distribution of distances, $p(x)$, is approximately normal, it will be a good approximation also at low values of ν .

Let us assume that $\bar{n}_\nu \simeq \tilde{n}_\nu$, irrespectively of q . This is a reasonable assumption, at least for low ν , since α is the key element determining the number of ways a set of edges can be concatenated. (For finite N , the approximation may break down at high ν and low q , because the maximum path length will be shorter in highly coherent graphs than in random ones.) In this case, multiplying \tilde{n}_ν by Eq. (1) yields the expected number of cycles of length ν :

$$\bar{m}_\nu = \frac{\tilde{q}}{q} e^{\tau\nu}, \quad (2)$$

where

$$\tau = \ln \alpha + \frac{1}{2\tilde{q}^2} - \frac{1}{2q^2}. \quad (3)$$

Eqs. (2) and (3) imply that the expected number of cycles of length ν in a graph can either grow exponentially with ν , when $\tau > 0$; or decrease exponentially, if $\tau < 0$. Which of these two regimes a given graph finds itself in is determined by the correlation between in- and out-degrees, $\alpha = \langle k^{in} k^{out} \rangle / \langle k \rangle$; the proportion of vertices with no incoming edges, B/N (via $\tilde{q} = \sqrt{N/B - 1}$); and the trophic coherence, given by q . Note that, as mentioned above, the definition of m_ν counts each cycle ν times, so the expected number of unique cycles is $\bar{m}_\nu^u = \tilde{q}/(q\nu) e^{\tau\nu}$.

Since $m_\nu = N\langle \lambda^\nu \rangle$, we have from Eq. (2) that the expected value of the ν -th moment of the distribution of eigenvalues is

$$\overline{\langle \lambda^\nu \rangle} = \frac{1}{N} \sum_i \bar{\lambda}_i^\nu = \frac{1}{N} \frac{\tilde{q}}{q} e^{\tau\nu}. \quad (4)$$

We can use this relation to obtain the expected value of the leading eigenvalue by considering the limit of large ν :

$$\lim_{\nu \rightarrow +\infty} \left(\sum_i \bar{\lambda}_i^\nu \right)^{\frac{1}{\nu}} = \bar{\lambda}_1 = e^\tau. \quad (5)$$

Note that the expressions for the configuration ensemble can be recovered by taking $q = \tilde{q}$, which, according to Eq. (3), implies $\tau = \ln \alpha$. Thus, the leading eigenvalue in the directed configuration ensemble is $\tilde{\lambda}_1 = \alpha = \langle k^{in} k^{out} \rangle / \langle k \rangle$. If the graph were symmetric ($k_i^{in} = k_i^{out} = k_i, \forall i$), we would have $\tilde{\lambda}_1 = \langle k^2 \rangle / \langle k \rangle$; while for the Erdős-Rényi ensemble we obtain $\lambda_1^{ER} = 1 + \langle k \rangle$.

These particular cases are in agreement with previous mean-field results for these ensembles [10, 11]. The expected distribution of eigenvalues is entirely defined by its full set of moments, as given by Eq. (4). For instance, the moment-generating function for graphs with given τ is $M_\lambda(t) = \sum_{\nu=0}^{\infty} \langle \lambda^\nu \rangle t^\nu / \nu! = (1 - N^{-1}) + N^{-1} \exp(te^\tau)$.

Fig. 1 displays the leading eigenvalues, λ_1 , against τ for a set of empirical directed networks. The ensemble average given by Eq. (3), shown with a line, provides a good estimate of the empirical values. Networks with negative τ have leading eigenvalues which are rarely greater than one, while those in the positive τ regime typically have much larger values. The inset shows the same results after self-edges have been removed. The agreement is now even better, since most of the networks in the negative τ regime now have $\lambda_1 = 0$. Many of the empirical networks used in Fig. 1 are food webs, but the dataset also includes examples of gene transcription, protein structure and neural networks; and electric circuit, international trade, P2P and linguistic networks. Details of each network are listed in SM. It is interesting to observe that while all the biological networks are significantly more trophically coherent than the configuration model expectation, the man-made networks are less so. The only exception to this rule is the electric circuit.

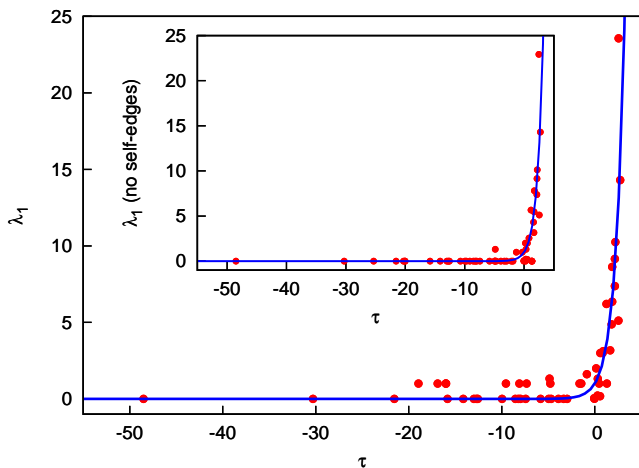


FIG. 1: Circles: Leading eigenvalues λ_1 of several real directed networks, against τ as given by Eq. (3). Line: Expected leading eigenvalue $\bar{\lambda}_1$ in the coherence ensemble, as given by Eq. (5). Inset: As in main panel, but after all self-edges (cycles of length $\nu = 1$) have been removed. Details for each of the empirical networks are listed in SM.

Directed acyclic graphs. Let us consider the probability that a graph randomly chosen from the coherence ensemble have exactly m_ν cycles of length ν . We shall assume that each path is an independent random event with two possible outcomes: with probability \bar{c}_ν it is a cycle, while with $1 - \bar{c}_\nu$ it is not. The number of cycles m_ν will therefore be binomially distributed: $p(m_\nu) =$

$\binom{\bar{n}_\nu}{m_\nu} \bar{c}_\nu^{m_\nu} (1 - \bar{c}_\nu)^{\bar{n}_\nu - m_\nu}$. We can use this distribution to obtain the probability that a network from the coherence ensemble have no directed cycles – i.e. that it be a directed acyclic graph (DAG): $P_{DAG} = \prod_{\nu=1}^{\infty} p(m_\nu = 0) = \prod_{\nu=1}^{\infty} \{1 - \alpha \tilde{q} (Lq)^{-1} \exp[\nu(\tilde{q}^{-2} - q^{-2})/2]\}^{L\alpha^{\nu-1}}$. Taking logarithms and considering graphs with sufficiently negative τ that we can use the approximation $\ln(1 - x) \simeq -x$, we have $\ln P_{DAG} \simeq -(\tilde{q}/q) \sum_{\nu=1}^{\infty} e^{\tau\nu}$; and, after performing the sum and some algebra,

$$P_{DAG} \simeq \exp \left[-\frac{\tilde{q}}{q} \frac{1}{(e^{-\tau} - 1)} \right]. \quad (6)$$

Therefore, as $\tau \rightarrow -\infty$, networks are almost always DAGs. By a similar reasoning we can obtain the probability that a graph in the coherence ensemble have only self-cycles:

$$P_{OSC} \simeq \exp \left[-\frac{\tilde{q}}{q} \frac{e^\tau}{(e^{-\tau} - 1)} \right] - P_{DAG}. \quad (7)$$

We note that these sums include small values of ν for which results are only approximate unless the distribution of trophic distances, $p(x)$, is Gaussian.

Fig. 2 is a scatter plot of our set of empirical networks according to $\ln \alpha + 1/(2\tilde{q}^2)$ and q . Each network is represented with a circle if it is a directed acyclic graph, with a diamond if its only cycles are self-edges, and with a square if it has any cycles of length greater than one. The curve $\tau = 0$ separates the two regimes. In the upper region ($\tau > 0$), all the networks have cycles of at least length two – and the correspondingly high values of λ_1 shown in Fig. 1. In the lower region ($\tau < 0$), such networks become increasingly rare as we move away from the $\tau = 0$ line, and most networks have only self-edges or no cycles at all. The only obvious outlier is the square in the bottom left hand corner. This is the gene transcription network of yeast, which has just one 2-cycle and one 3-cycle involving both the genes in the 2-cycle.

Discussion. We have shown that a directed network can belong to either of two regimes characterised by fundamentally different cycle structures, depending on the sign of a single parameter, $\tau = \ln(\langle k^{in} k^{out} \rangle / \langle k \rangle) + (\tilde{q}^{-2} - q^{-2})/2$, where q and \tilde{q} give the trophic coherence for the network and for the corresponding configuration model. Since the expected number of cycles of length ν is proportional to $e^{\tau\nu}$, positive τ implies an exponentially growing number of cycles with length, while for negative τ the probability of finding cycles is vanishing. This, in turn, has a crucial effect on the spectral properties of graphs: in particular, the expected value of the leading eigenvalue of the adjacency matrix is $\bar{\lambda}_1 = e^\tau$. A corollary is that graphs drawn randomly from the negative τ regime have a high probability of being directed acyclic graphs, the main requisite for qualitative stability [12].

The fact that many biological networks have non-trivially few cycles (often called feedback loops) has recently been attributed to considerations of robustness

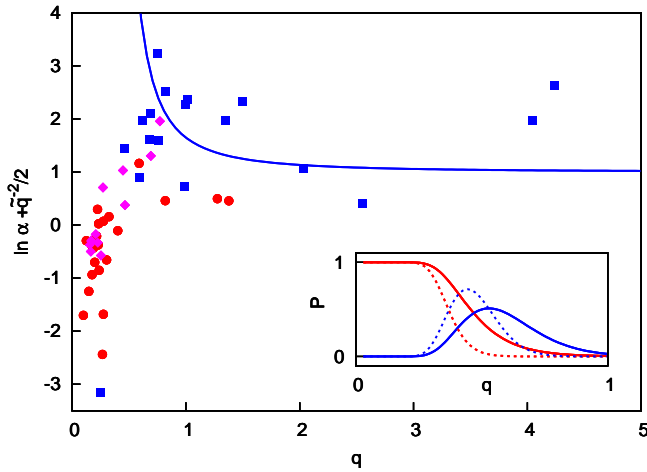


FIG. 2: Scatter plot of several empirical networks, according to $\ln \alpha + \tilde{q}^{-2}/2$ and q . Each network is represented with a blue square if it has no cycles, with a lilac diamond if its only cycles are of length one (self-edges), or with a red circle if it has higher order cycles. The $\tau = 0$ line is also shown. Details for each of the empirical networks are listed in SM. Inset: Probabilities of a network in the coherence ensemble being a directed acyclic graph (monotonic or red lines), or having only self-edges (non-monotonic or blue lines), as a function of trophic coherence, as given by Eqs. (6) and (7) with $\alpha = 1$. Solid and dashed lines are for $N/B = 10$ and $N/B = 100$, respectively.

[13], stability [14], and to an “inherent directionality” [15]. Our results are compatible with the latter, since network directionality is another consequence of trophic coherence (that is, since the distribution of distances $p(x)$ is centred at 1 and has variance q^2 , the expected number of edges with $x < 0$ is $L \int_{-\infty}^0 p(x) dx$, a monotonously increasing function of q). However, our analysis indicates that any network formation processes which tended to induce a certain coherence – such as vertexes having specific roles – would confer the properties of a low or negative τ on a system without necessarily being the result of optimization.

Our results provide expected values for what we have called the coherence ensemble – the set of directed graphs with given degree sequence and trophic coherence. This does not place bounds on the possible values a given network can exhibit, but suggests, instead, which should be the correct null-model to use. For instance, there are two genes in the transcription network of yeast which are involved in both a 2-cycle and a 3-cycle. That in a network of 688 vertices and 1079 edges there should be no other

cycles than these might seem puzzling given only the degree sequence. But if we take trophic coherence into account, we find that the probability of observing any cycles of length greater than one is less than $2 \cdot 10^{-6}$. We should look, rather, at what role these highly improbable feedback loops might play. In any case, our work suggests that the trophic structure of directed networks may provide insights into their function and dynamics. For instance, classifying genes, neurons, metabolites, protein configurations, economic agents or even words according to their trophic levels may help us understand the systems they form part of, just as ecologists have long found to be the case with the species making up ecosystems.

Acknowledgements. Many thanks to M.A. Muñoz and V. Domínguez-García for a fruitful collaboration from which some of these ideas sprouted. We are grateful to I. Johnston, M. Ibáñez Berganza and J. Klaise for useful discussions. Thanks also to J. Dunne, U. Jacob, R.M. Thompson, C.R. Townsend, U. Alon, M.E.J. Newman, W. de Nooy, and J. Leskovec for providing data or making them available online (see SM.)

* S.Johnson.2@warwick.ac.uk

- [1] E. P. Wigner, Ann. Math. **62**, 548 (1955).
- [2] M. Fiedler, Czech. Math. J **23**, 298 (1973).
- [3] M. E. J. Newman, Proc. Natl. Acad. Sci. USA **103**, 8577 (2006).
- [4] B. Bollobás, C. Borgs, J. Chayes, and O. Riordan, Ann. Prob. **38**, 150 (2010).
- [5] R. M. May, Nature **238**, 413 (1972).
- [6] A. Barrat, M. Barthélemy, and A. Vespignani, *Dynamical Processes on Complex Networks* (Cambridge University Press, Cambridge, 2008).
- [7] A. Arenas, A. Díaz-Guilera, J. Kurths, Y. Moreno, and C. Zhou, Phys. Rep. **469**, 93 (2008).
- [8] S. Johnson, V. Domínguez-García, L. Donetti, and M. A. Muñoz, Proc. Natl. Acad. Sci. USA **111**, 17923 (2014).
- [9] H. Kim, C. I. Del Genio, K. E. Bassler, and Z. Toroczkai, New J. Phys. **14**, 023012 (2012).
- [10] F. Chung, L. Lu, and V. Vu, Proc. Natl. Acad. Sci. USA **100**, 6313 (2003).
- [11] R. R. Nadakuditi and M. E. J. Newman, Phys. Rev. E **87**, 012803 (2013).
- [12] R. M. May, Ecology **54**, 638 (1973).
- [13] L. Albergante, J. J. Blow, and T. J. Newman, eLife **3**, e02863 (2014).
- [14] J. J. Borrelli, Oikos (2015).
- [15] V. Domínguez-García, S. Pigolotti, and M. A. Muñoz, Sci. Rep. **4**, 7497 (2014).

Supplemental Material for “Spectra and cycle structure of trophically coherent graphs”

Samuel Johnson^{1*} and Nick S. Jones²

¹Warwick Mathematics Institute, and Centre for Complexity Science,
University of Warwick, Coventry CV4 7AL, United Kingdom.

²Department of Mathematics, Imperial College London,
London SW7 2AZ, United Kingdom.

*E-mail: S.Johnson.2@warwick.ac.uk

1 Trophic coherence in the configuration model

In the main text we use a mean-field approximation to obtain the trophic coherence of networks in the configuration ensemble, which is found to depend only on the proportion of vertices with no in-coming edges, B/N :

$$\tilde{q} = \sqrt{\frac{N}{B} - 1}. \quad (1)$$

Figure 1 shows the values of q obtained for simulated networks and contrasts these with the prediction of Eq. (1). Two of the network types are scale free; that is, in- and out-degrees are drawn independently from distributions $p(k_{in}) \sim k_{in}^{-\gamma}$ and $p(k_{out}) \sim k_{out}^{-\gamma}$, with the constraint that B vertices have $k_{in} = 0$, and then wired according to the directed configuration model. Results for $\gamma = 2.5$ and $\gamma = 3$ are shown. The other networks are directed random graphs, generated like Erdős-Rényi graphs but again with the constraint that there be B basal vertices. As can be observed, Eq. (1) accurately provides the expected value of q in these graphs, irrespectively of degree heterogeneity.

2 Network data

In the main text we assess the validity of our analytical results through comparisons with a set of empirical directed networks. Most of these are available online, but a few of them were shared with us in private correspondence (see Acknowledgements). Below we list the most relevant details for each of these networks. Table 1 is for 42 food webs (networks used to describe trophic interactions in ecosystems, with each vertex a species and directed edges going from prey to predators). Table 2 is for another six biological networks: two gene transcription networks, a neural network, and three protein structure networks. Table 3 is for five artificial networks: an electric circuit, a P2P file sharing network, two networks of trade between nations, and a network of concatenated English words.

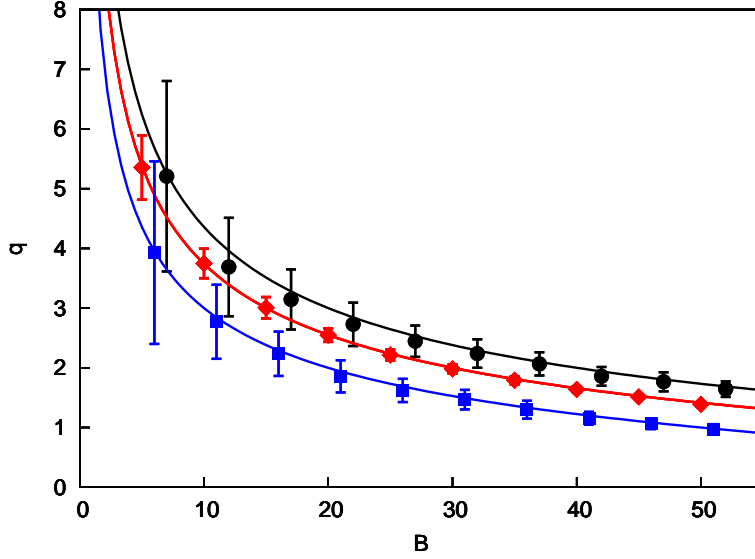


Figure S 1. Trophic coherence, as measured by q , against number of basal vertices B , for simulated networks with number of vertices N and mean degree $\langle k \rangle = 10$. Black circles: scale-free networks with exponent $\gamma = 2.5$, and $N = 200$. Red diamonds: random graphs with $N = 150$. Blue squares: scale-free networks with $\gamma = 3$, and $N = 100$. The scale-free networks are generated with the configuration model, while the random graphs are produced with a modification of the Erdős-Rényi model such that the number of basal vertices is fixed. Lines in each case are for the corresponding prediction given by Eq. (1).

For each network, we list the number of vertices, N , and the mean degree, $\langle k \rangle$. The branching factor, $\alpha = \langle k^{in} k^{out} \rangle / \langle k \rangle$, is displayed as a fraction of the mean degree; thus, values greater (smaller) than one indicate that in- and out-degrees are positively (negatively) correlated. The incoherence parameter q is the standard deviation of the distribution of trophic distances, $p(x)$, as defined in the main text and in Ref. [1]: the closer q is to zero, the more trophically coherent the network. This parameter is also displayed as a fraction of the corresponding expected value for a random graph (as obtained in the main text), \tilde{q} . Values greater (smaller) than one indicate that networks are less (more) trophically coherent than the null expectation. The parameter

$$\tau = \ln \alpha + \frac{1}{2\tilde{q}^2} - \frac{1}{2q^2}$$

determines whether the number of cycles will grow ($\tau > 0$) or decrease ($\tau < 0$) exponentially with cycle length; and is therefore key to many network properties, as described in the main text. The leading eigenvalue of the adjacency matrix, λ_1 , is related to many structural and dynamical features of networks. In the coherence ensemble, it is related to τ via $\lambda_1 = e^\tau$ (see main text).

Food web	N	B	$\langle k \rangle$	$\alpha/\langle k \rangle$	q	q/\tilde{q}	τ	λ_1	Reference
Benguela Current	29	2	7	0.72	0.762	0.207	0.8	3	[2]
Berwick Stream	79	37	3.04	1.37	0.176	0.165	-16.27	0	[3, 4, 5]
Blackrock Stream	87	50	4.31	0.76	0.187	0.217	-13.4	0	[3, 4, 5]
Bridge Brook Lake	25	8	4.28	0.72	0.59	0.404	-0.08	2	[6]
Broad Stream	95	54	5.95	0.84	0.165	0.189	-17.55	1	[3, 4, 5]
Canton Creek	102	54	6.83	0.18	0.157	0.167	-19.52	1	[7]
Caribbean Reef	50	3	11.12	0.91	0.992	0.251	1.84	8.63	[8]
Caribbean (2005)	261	29	14.43	0.32	0.772	0.273	1.24	1	[9]f
Catlins Stream	49	15	2.24	0.74	0.2	0.133	-12.8	0	[3, 4, 5]
Chesapeake Bay	31	5	2.19	0.73	0.465	0.204	-1.74	1	[10, 11]
Coachella Valley	29	3	9.03	0.85	1.344	0.457	1.82	6.35	[12]
Coweeta (17)	71	38	2.08	0.23	0.238	0.255	-8.57	0	[3, 4, 5]
Coweeta (1)	58	28	2.17	1.83	0.303	0.293	-5.16	0	[3, 4, 5]
Dempsters (Au)	86	49	4.83	0.52	0.226	0.261	-8.76	1	[3, 4, 5]
Dempsters (Sp)	97	54	5.55	0.2	0.125	0.14	-30.92	0	[3, 4, 5]
Dempsters (Su)	107	50	9.03	0.3	0.271	0.254	-5.21	1	[3, 4, 5]
El Verde Rainforest	155	28	9.74	1.23	1.017	0.477	2.11	10.25	[13]
German Stream	86	50	4.1	0.2	0.209	0.246	-10.25	1	[3, 4, 5]
Healy Stream	96	47	6.6	0.28	0.224	0.22	-8.7	0	[3, 4, 5]
Kyeburn Stream	98	58	6.42	0.36	0.177	0.213	-14.86	0	[3, 4, 5]
LilKyeburn Stream	78	42	4.81	0.38	0.233	0.252	-8.01	0	[3, 4, 5]
Little Rock Lake	92	12	10.84	0.81	0.687	0.266	1.19	6.2	[14]
Lough Hyne	349	49	14.66	0.33	0.618	0.25	0.83	3.12	[15, 16]
Martins Stream	105	48	3.27	0.29	0.324	0.297	-3.76	0	[3, 4, 5]
Narrowdale Stream	71	28	2.18	0.25	0.254	0.205	-7.65	1	[3, 4, 5]
NE Shelf	79	2	17.76	0.71	0.82	0.132	1.81	4.87	[17]
North Col Stream	78	25	3.09	0.35	0.275	0.189	-6.06	0	[3, 4, 5]
Powder Stream	78	32	3.44	0.41	0.215	0.179	-10.32	0	[3, 4, 5]
Scotch Broom	85	1	2.62	1.07	0.447	0.049	-1.46	1	[18]
Skipwith Pond	25	1	7.88	0.66	0.677	0.138	0.57	3	[19]
St Marks Estuary	48	6	4.6	0.86	0.692	0.262	0.4	1	[20]
St Martin Island	42	6	4.88	0.71	0.589	0.241	-0.11	0.01	[21]
Stony Stream	109	61	7.61	0.19	0.169	0.19	-16.62	1	[22]
Stony Stream 2	113	64	7.36	0.33	0.168	0.192	-16.67	1	[3, 4, 5]
Sutton (Au)	83	52	4.04	0.22	0.148	0.192	-22.4	0	[3, 4, 5]
Sutton (Sp)	79	55	4.95	0.38	0.1	0.151	-49.66	0	[3, 4, 5]
Sutton (Su)	94	70	4.51	0.55	0.275	0.47	-5.36	0	[3, 4, 5]
Troy Stream	78	41	2.32	0.36	0.187	0.197	-13.55	0	[3, 4, 5]
UK Grassland	61	8	1.59	0.61	0.402	0.156	-3.05	0	[23]
Venlaw Stream	69	33	2.71	0.44	0.229	0.219	-8.99	0	[3, 4, 5]
Weddell Sea	483	61	31.81	0.19	0.748	0.284	2.49	23.56	[24]
Ythan Estuary	82	5	4.82	0.91	0.457	0.116	-0.89	1.62	[25]

Table S 1. Details of 42 food webs used in the main text. Columns are for number of vertices N , number of basal vertices B , mean degree $\langle k \rangle$, branching factor relative to mean degree, incoherence parameter, incoherence parameter relative to the random expectation, parameter τ (as defined in main text), leading eigenvalue, and references. Many of these networks can be found online at: https://www.nceas.ucsb.edu/interactionweb/html/thomps_towns.html

Network (biological)	N	B	$\langle k \rangle$	$\alpha/\langle k \rangle$	q	q/\tilde{q}	τ	λ_1	Reference
Gene transcription (E. coli)	423	317	1.23	0.16	0.267	0.462	-6.45	0	[26]
Gene transcription (Yeast)	688	557	1.57	1.37	0.249	0.513	-6.99	1.32	[26]
Neural (C. elegans)	306	12	7.66	0.12	1.494	0.302	2.15	9.15	[27, 28]
Protein structure (1A4J)	95	6	2.24	0.18	1.277	0.332	0.26	0.22	[26]
Protein structure (1AOR)	99	20	2.14	0.49	1.377	0.693	0.45	0.18	[26]
Protein structure (1EAW)	53	7	2.32	0.4	0.818	0.319	-0.14	0.04	[26]

Table S 2. Details of six biological networks used in the main text: two gene transcription networks, a neural network, and three protein structure networks. Columns as in Table

1. The gene transcription and protein structure networks are available online at: <http://wws.weizmann.ac.il/mcb/UriAlon/download/collection-complex-networks>; and the neural network can be found at: <http://www-personal.umich.edu/~mejn/netdata/>

Network (artificial)	N	B	$\langle k \rangle$	$\alpha/\langle k \rangle$	q	q/\tilde{q}	τ	λ_1	Reference
Electric circuit (s38_st)	512	1	1.6	1.3	2.552	0.113	0.32	1.32	[26]
P2P (Gnutella 08)	6301	3836	3.3	1.12	0.984	1.227	1.77	5.12	[29, 30]
Trade (manufactured goods)	24	2	12.92	0.53	4.24	1.278	2.69	14.3	[31]
Trade (minerals, fuels, etc.)	24	3	5.96	0.86	4.042	1.528	2.09	7.38	[31]
Words (Green Eggs and Ham)	50	16	2.02	0.93	2.037	1.398	1.42	3.17	[32]

Table S 3. Details of five artificial networks used in the main text: an electric circuit, a P2P file sharing network, two networks of trade between nations, and the network of concatenated words in Dr. Seuss' masterpiece Green Eggs and Ham. Columns as in Table 1. The electric circuit is available at: <http://wws.weizmann.ac.il/mcb/UriAlon/download/collection-complex-networks>; the P2P network can be found at: <https://snap.stanford.edu/data/p2p-Gnutella08.html>; the trade networks are here: <http://vlado.fmf.uni-lj.si/pub/networks/data/esna/metalWT.htm>; and the network of words is available upon request from s.johnson.2@warwick.ac.uk.

References

- [1] S. Johnson, V. Domínguez-García, L. Donetti, and M. A. Muñoz, “Trophic coherence determines food-web stability,” *Proc. Natl. Acad. Sci. USA*, vol. 111, no. 50, pp. 17923–17928, 2014.
- [2] P. Yodzis, “Local trophodynamics and the interaction of marine mammals and fisheries in the benguela ecosystem,” *Journal of Animal Ecology*, vol. 67, no. 4, pp. 635–658, 1998.
- [3] R. M. Thompson and C. R. Townsend, “Impacts on stream food webs of native and exotic forest: An intercontinental comparison,” *Ecology*, vol. 84, pp. 145–161, 2003.
- [4] R. M. T. and C. R. Townsend, “Energy availability, spatial heterogeneity and ecosystem size predict food-web structure in stream,” *Oikos*, vol. 108, p. 137–148, 2005.
- [5] Townsend, Thompson, McIntosh, Kilroy, Edwards, and Scarsbrook, “Disturbance, resource supply, and food-web architecture in streams,” *Ecology Letters*, vol. 1, no. 3, pp. 200–209, 1998.
- [6] K. Havens, “Scale and structure in natural food webs,” *Science*, vol. 257, no. 5073, pp. 1107–1109, 1992.
- [7] Townsend, Thompson, McIntosh, Kilroy, Edwards, and Scarsbrook, “Disturbance, resource supply, and food-web architecture in streams,” *Ecology Letters*, vol. 1, no. 3, pp. 200–209, 1998.
- [8] S. Opitz, “Trophic interactions in Caribbean coral reefs,” *ICLARM Tech. Rep.*, vol. 43, p. 341, 1996.
- [9] J. Bascompte, C. Melián, and E. Sala, “Interaction strength combinations and the overfishing of a marine food web,” *Proceedings of the National Academy of Sciences of the United States of America*, vol. 102, no. 15, pp. 5443–5447, 2005.
- [10] R. E. Ulanowicz and D. Baird, “Nutrient controls on ecosystem dynamics: the chesapeake mesohaline community,” *Journal of Marine Systems*, vol. 19, no. 1–3, pp. 159 – 172, 1999.
- [11] L. G. Abarca-Arenas and R. E. Ulanowicz, “The effects of taxonomic aggregation on network analysis,” *Ecological Modelling*, vol. 149, no. 3, pp. 285 – 296, 2002.
- [12] G. Polis, “Complex trophic interactions in deserts: an empirical critique of food-web theory,” *Am. Nat.*, vol. 138, pp. 123–125, 1991.
- [13] R. B. Waide and W. B. R. (eds.), *The Food Web of a Tropical Rainforest*. Chicago: University of Chicago Press, 1996.
- [14] N. D. Martinez, “Artifacts or attributes? Effects of resolution on the Little Rock Lake food web,” *Ecol. Monogr.*, vol. 61, pp. 367–392, 1991.

- [15] J. Riede, U. Brose, B. Ebenman, U. Jacob, R. Thompson, C. Townsend, and T. Jonsson, “Stepping in Elton’s footprints: a general scaling model for body masses and trophic levels across ecosystems,” *Ecology Letters*, vol. 14, pp. 169–178, 2011.
- [16] A. Eklöf, U. Jacob, J. Kopp, J. Bosch, R. Castro-Urgal, B. Dalsgaard, N. Chacoff, C. deSassi, M. Galetti, P. Guimaraes, S. Lomáscolo, A. Martín González, M. Pizo, R. Rader, A. Rodrigo, J. Tylianakis, D. Vazquez, and S. Allesina, “The dimensionality of ecological networks,” *Ecology Letters*, vol. 16, pp. 577–583, 2013.
- [17] J. Link, “Does food web theory work for marine ecosystems?,” *Mar. Ecol. Prog. Ser.*, vol. 230, pp. 1–9, 2002.
- [18] J. Memmott, N. D. Martinez, and J. E. Cohen, “Predators, parasitoids and pathogens: species richness, trophic generality and body sizes in a natural food web,” *J. Anim. Ecol.*, vol. 69, pp. 1–15, 2000.
- [19] P. H. Warren, “Spatial and temporal variation in the structure of a freshwater food web,” *Oikos*, vol. 55, pp. 299–311, 1989.
- [20] R. R. Christian and J. J. Luczkovich, “Organizing and understanding a winter’s Seagrass foodweb network through effective trophic levels,” *Ecol. Model.*, vol. 117, pp. 99–124, 1999.
- [21] L. Goldwasser and J. A. Roughgarden, “Construction of a large Caribbean food web,” *Ecology*, vol. 74, pp. 1216–1233, 1993.
- [22] Townsend, Thompson, McIntosh, Kilroy, Edwards, and Scarsbrook, “Disturbance, resource supply, and food-web architecture in streams,” *Ecology Letters*, vol. 1, no. 3, pp. 200–209, 1998.
- [23] N. D. Martinez, B. A. Hawkins, H. A. Dawah, and B. P. Feifarek, “Effects of sampling effort on characterization of food-web structure,” *Ecology*, vol. 80, p. 1044–1055, 1999.
- [24] U. Jacob, A. Thierry, U. Brose, W. Arntz, S. Berg, T. Brey, I. Fetzer, T. Jonsson, K. Mintenbeck, C. Möllmann, O. Petchey, J. Riede, and J. Dunne, “The role of body size in complex food webs,” *Advances in Ecological Research*, vol. 45, pp. 181–223, 2011.
- [25] M. Huxham, S. Beaney, and D. Raffaelli, “Do parasites reduce the chances of triangulation in a real food web?,” *Oikos*, vol. 76, pp. 284–300, 1996.
- [26] R. Milo, S. Itzkovitz, N. Kashtan, R. Levitt, S. Shen-Orr, I. Ayzenshtat, M. Sheffer, and U. Alon, “Superfamilies of evolved and designed networks,” *Science*, vol. 303, no. 5663, pp. 1538–1542, 2004.
- [27] J. G. White, E. Southgate, J. N. Thompson, and S. Brenner, “The structure of the nervous system of the nematode *Caenorhabditis elegans*,” *Phil. Trans. R. Soc. London*, vol. 314, pp. 1–340, 1986.
- [28] D. J. Watts and S. H. Strogatz, “Collective dynamics of ‘small-world’ networks,” *Nature*, vol. 393, pp. 440–442, 1998.

- [29] J. Leskovec, J. Kleinberg, and C. Faloutsos, “Graph evolution: Densification and shrinking diameters,” *ACM Transactions on Knowledge Discovery from Data*, vol. 1, 2007.
- [30] M. Ripeanu, I. Foster, and A. Iamnitchi, “Mapping the gnutella network: Properties of large-scale peer-to-peer systems and implications for system design,” *IEEE Internet Computing Journal*, 2002.
- [31] W. de Nooy, A. Mrvar, and V. Batagelj, *Exploratory Social Network Analysis with Pajek*. Cambridge: Cambridge University Press, 2004.
- [32] Dr Seuss, *Green Eggs and Ham*. Random House, 1960.